lite and granulite facies rocks has yielded an age of 2.92 ± 0.05 gigayears (mean ± 2 standard deviations) (P. J. Hamilton, S. R. Carter, N. M. Evensen, R. K. O'Nions, J. Tarney, in preparation). The granulites have very low Rb/Sr ratios (0.005 to 0.009) and Sm/Nd ratios less than 0.31, whereas the amphibolites facies have similar Sm/Nd ratios but much higher Rb/Sr ratios (0.07 to 0.19).

20. The North Atlantic Tertiary province was formed during the initiation of sea-floor spreading between Greenland and Eurasia and comprises plateau lavas and central intrusive complexes of granite, gabbro, and peridotite. Lavas cover approximately 2000 km^2 and have a present stratigraphic thickness of 2000 m in Mull and about 1000 m in Skye. Alkali olivine basalts predominate but are associated with tholeiites, hawaiites, mugearites, and trachytes. Recent K-Ar studies on samples from Mull indicate a mean extrusion age of about 60 million years for the lavas of this province (*22*). The youngest reliable age obtained on intrusive centers in Skye by the Rb-Sr method is 55 million years (*21*). Samples were collected from areas outside the known zones of hydrothermal alteration.
21. S. Moorbath and J. D. Bell, *J. Petrol.* **6**, 37 (1965).
22. R. D. Beckinsale, R. J. Pankhurst, R. R. Skelhorn, J. N. Walsh, *Contrib. Mineral. Petrol.* **66**, 415 (1978).
23. The Rb, Sr, Sm, and Nd were separated from spiked and unspiked sample portions by ion exchange techniques. Concentrations and isotopic ratios were determined on a Vacuum Generators Micromass 30. The chemical and instrumental techniques have been described previously (*9*).
24. The Δ parameter (for Sm-Nd systematics) is defined by

$$\Delta\text{ND}(\%) = \frac{R_{\text{single stage}} - R_{\text{bulk earth}}}{R_{\text{bulk earth}}} \times 10^2$$

where $R = {}^{147}\text{Sm}/{}^{144}\text{Nd}$ and

$${}^{147}\text{Sm}/{}^{144}\text{Nd}_{\text{single stage}} = \frac{{}^{143}\text{Nd}/{}^{144}\text{Nd}_{\text{measured}} - 0.50682}{\exp(\lambda^{147} \times T) - 1}$$

where $T = 4.55$ gigayears. The parameter ΔSR is defined analogously.

25. R. K. O'Nions, S. R. Carter, R. S. Cohen, N. M. Evensen, P. J. Hamilton, *Nature (London)* **273**, 435 (1978).
26. S. Moorbath and H. Welke, *Earth Planet. Sci. Lett.* **5**, 217 (1968).
27. In general, contamination may occur either by bulk assimilation of contaminant material or by differential incorporation of low melting point phases from the contaminant rocks, in a manner equivalent to the mixing of partial melts of crustal material with the ascending magma. Since Rb, Sr, and the rare earths tend to be concentrated within early melting phases, the latter mechanism is more efficient at extracting these elements for a given loss of heat from the magma.
28. R. S. Thorpe, P. J. Potts, M. B. Sarre, *Earth Planet. Sci. Lett.* **36**, 111 (1977).
29. H. P. Taylor, Jr., and R. W. Forrester, *J. Petrol.* **12**, 465 (1971).
30. The well-known stability of rare earths during weathering and alteration processes (references below) and the markedly different Nd isotope compositions of Lewisian gneisses and the least-contaminated Tertiary basic volcanics suggest that Nd isotope studies may aid in the resolution of these various viewpoints concerning the origin of the acid intrusives [A. G. Herrman, M. J. Potts, D. Knake, *Contrib. Mineral. Petrol.* **44**, 1 (1974); R. Kay, N. J. Hubbard, P. W. Gast, *J. Geophys. Res.* **75**, 1585 (1970); F. A. Frey, M. A. Haskin, J. A. Poetz, L. A. Haskin, *ibid.* **73**, 6085 (1968); J. D. Smewing and P. J. Potts, *Contrib. Mineral. Petrol.* **57**, 245 (1976); R. K. O'Nions and R. J. Pankhurst, *Earth Planet. Sci. Lett.* **31**, 255 (1976); P. J. Hamilton, R. K. O'Nions, N. M. Evensen, *ibid.* **36**, 263 (1977); P. J. Hamilton *et al.* (*10*).
31. Marscoite is a hybrid, intermediate, intrusive rock thought to be the result of mixing between basic and acidic magmas [L. R. Wager, E. A. Vincent, G. M. Brown, J. D. Bell, *Philos. Trans. R. Soc. London Ser. A* **257**, 273 (1965)].
32. W. I. Ridley and J. Tarney kindly supplied some of the samples. G. Weisselman and R. Cohen are thanked for their technical help and J. Tarney for valuable discussions. Supported by NSF grant EAR-75-20891. This is Lamont-Doherty Geological Observatory Contribution No. 2743.

7 June 1978; revised 28 August 1978

Shark Skin: Function in Locomotion

Abstract. *Hydrostatic pressure under the skin of sharks varies with swimming speed. Stress in the skin varies with the internal pressure, and the skin stress controls skin stiffness. Locomotory muscles attach to the skin which is thus a whole-body exotendon whose mechanical advantage in transmitting muscular contraction is greater than that of the endoskeleton.*

Sharks, we find, are supported in part by hydrostatic pressure. Their internal pressure increases more than tenfold from slow to fast swimming. This increase in pressure causes the skin to become stiffer. Because the skin shortens and lengthens with the muscles when the fish bends and because the muscles are as securely attached to the skin as they are to the backbone, the skin acts as an external tendon by transmitting muscular force and displacement to the tail.

We measured internal hydrostatic pressure of 7 to 14 kN m^{-2} just under the skin in a lemon shark (*Negaprion brevirostris*, 87 cm long) resting on the tank floor (*1*). While swimming slowly, the shark bent its body in left and right bends of 38 cm radius of curvature, and the pressure varied between 20 and 35 kN m^{-2}. During bursts of fast swimming, tighter bends of 20 cm radius were produced, and pressure rose to 200 kN m^{-2} once each tail beat—that is, the pressure rose on both concave and convex sides of the fish.

The cause of the pressure increase is unknown, and it may be derived from more than one source: change in muscle surface area compared to skin area or an active increase in blood pressure. The latter might be bought about by the posterior displacement of blood from the cardinal sinuses by contraction of the constrictor muscles that encircle the body behind the head (*2*).

The white, inner, thickest layer of shark skin is a sheath of fabric cut on the bias: it consists of layers of collagen fibers that lie in helices around the shark's body (*3*). In alternating layers, the fibers describe right- and left-handed helices. The angle these helices make with the long axis of the shark is called the fiber angle, and in all selachians that we studied (*4*) and studied by others (*3*), it varies between 50° and 70° between the pectoral and anal fins and between 45° and 50° in the thin caudal peduncle just in front of the tail (Fig. 1). Collagen fibers in shark skin, which are mechanically similar to those in mammalian tendon (*5*), are very stiff in tension but flexible in bending. Pressurized cylinders, such as the bodies of worms and sharks, are reinforced with helically wound collagen fibers. This allows flexibility for undulation and reinforces the body wall against embolisms and bursting (*6*). It also prevents wrinkling on the concave side.

Hydrostatic pressure of 21 kN m^{-2} in the cruising shark induces a circumferential stress of 0.3 MN m^{-2} in the skin (*7*). When we held a constant circumferential stress of 0.3 MN m^{-2} in a specimen of shark skin while pulling it longitudinally in a biaxial testing machine (*8*), we found (Fig. 2, lower curve) a great longitudinal extensibility of the skin. Results of an experiment in which we held circumferential stress at the fast swimming value of 2.8 MN m^{-2} (Fig. 2, upper curve) show that the stress in the unstretched skin at zero extension has increased 13-fold and that a given longitudinal extension requires very much more stress than it does in the lower pressure, slower swimming situation.

The slope of such a curve at any point is a measure of the stiffness of the material under those conditions. In slowly swimming sharks, we measured ±10 percent longitudinal and ±3 percent circumferential extensions (*9*). At pressures recorded at different speeds, the stiffness of the shark skin is thus apparently 0.8 MN m^{-2} for the slowly swimming shark and 3.0 MN m^{-2} for the fast one. The area under the force-extension curve is a measure of the energy required for and recovered from skin deformation, and the area between the loading and unloading parts of the curve is a measure of the energy lost during the deformation cycle. The energy stored by the skin is much higher over the physiological range of ±15 percent extensions occurring during fast swimming than it is over the ±10 percent extensions occurring during slow swimming (Fig. 2). Large energy losses occur only when the skin is stretched more than 20 percent. The very small energy loss over the physiological extensions support the notion that viscous reorganization of interfiber matrix is not important in the living fish.

If the mechanical properties of shark skin were due simply to the properties of the collagen fiber array without contributions from an interfiber matrix or other morphological features, the instantaneous ratio of circumferential to longitudinal stresses at any point on the shark would be equal to the square of the tangent of the fiber angle. Such a predictive curve for the slowly swimming shark would connect the points (crosses) on the lower curve in Fig. 2. We infer that, in the slowly swimming shark, change in the fiber angle determines the stress-extension behavior of the skin.

These results show that skin stiffness and the energy stored in shark skin depend on the amount by which the skin is prestressed by internal hydrostatic pressure at the time that it is extended. Muscle contracting isometrically at near maximum extension generates less force than does muscle that is shortening actively at less than maximum extension (*10*). In the fast swimming shark, energy stored elastically in the stretched skin on the convex side may be released when muscles are relaxed on the concave side. Coming at a time when the extended muscle can produce relatively little tension, this elastic recoil would accelerate unbending of the fish as muscles on the convex side begin their contraction phase. This would increase power output at the start of a fast swimming stroke.

Torque tending to twist the shark about its long axis during swimming is, we believe, due to asymmetric distribution of thrust produced by the heterocercal tail. Twisting of the tail during a power stroke would reduce its thrust-producing area. Torsional stiffness is proportional to J, the polar second moment of area of the cross section. For a solid cylinder of radius r, $J = r^4\pi/4$. From this we can see that the best way to stiffen a cylinder against torsion would be to add a stiff material as far as possible from the center in order to take advantage of the r^4 term. Since twisted cylinders of homogeneous material fail by splitting at 45° to their long axis (*6*), the best design for torsional stiffness in the shark's caudal peduncle would be collagen fibers in the skin wrapped at 45° to the body's long axis. This is what we found.

To assess the torsional stiffness conveyed to the shark's body by the skin and the inert muscle, we clamped the caudal fin of a dead dusky shark (2.18 m long) to a board and twisted it about the shark's long axis while recording the angular displacement achieved by applied torques. We then cut through the skin round the base of the tail and repeated the measurements. A 40° twist of the intact tail required a 4.8 N·m torque. The same twist after the skin was cut required 2.4 N·m while only 0.7 N·m was required to twist the backbone alone through 40°. Even though skin thickness (2 mm) is 6 percent of muscle thickness (32 mm) at that point, the skin accounts for half the passive resistance to twisting in the dead shark. The shear stiffness of both skin and muscle of a pressurized, swimming shark will be even greater than that of a dead shark, but the structure and position of the shark's skin suit it well for conveying torsional stiffness to the shark.

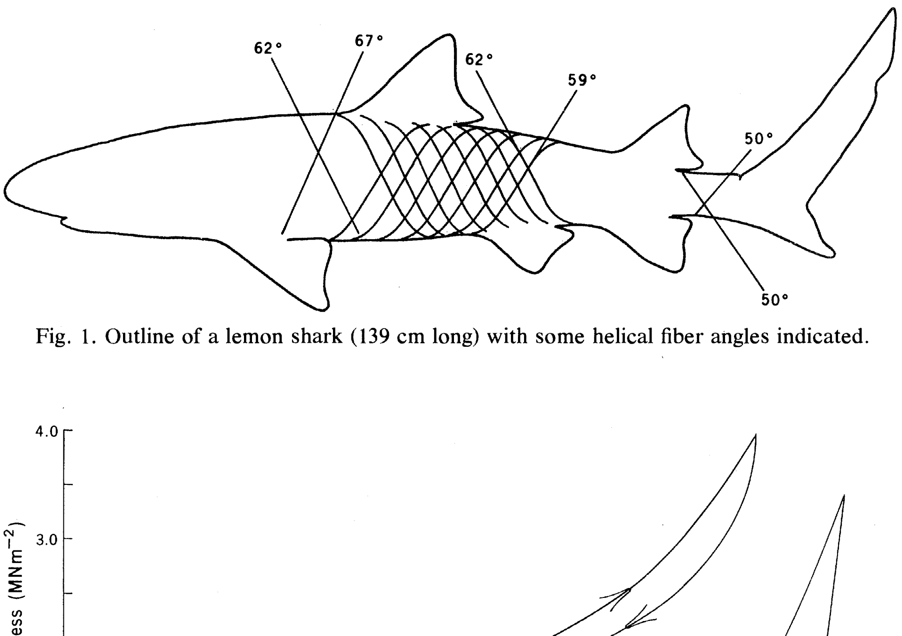

Fig. 1. Outline of a lemon shark (139 cm long) with some helical fiber angles indicated.

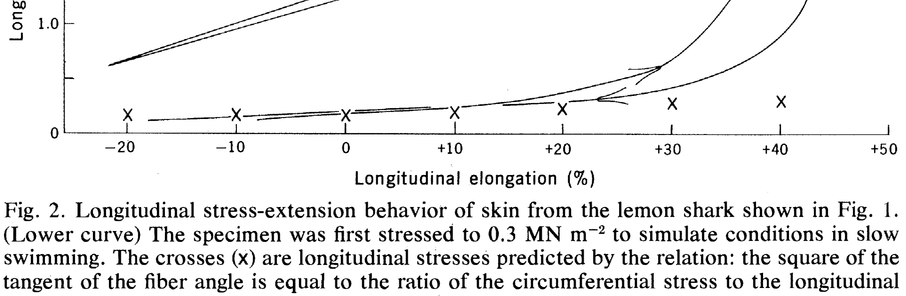

Fig. 2. Longitudinal stress-extension behavior of skin from the lemon shark shown in Fig. 1. (Lower curve) The specimen was first stressed to 0.3 MN m^{-2} to simulate conditions in slow swimming. The crosses (x) are longitudinal stresses predicted by the relation: the square of the tangent of the fiber angle is equal to the ratio of the circumferential stress to the longitudinal stress. (Upper curve) The specimen was first stressed to 2.8 MN m^{-2} to simulate conditions in fast swimming. Rising and falling arrows indicate loading and unloading, respectively.

Let us now consider the skin as part of the skeletomuscular locomotory system of the shark. It is difficult to clean the muscle from the skin of any freshly caught fish because the outermost muscle fibers are attached directly to the skin. Locomotory muscles in fishes are segmented. Within each segment, muscle fibers are oriented longitudinally and attach by their ends to the thin collagenous myosepta that insert centrally onto the midsagittal connective tissue septum and peripherally onto the skin. Because of this arrangement and the fact that the skin is the tension-resisting container of hydrostatic pressure involved in swimming, shark skin must be considered to be an exoskeletal structure in the same category with the cuticles of nematodes and caterpillars.

Implicit in the apparently universal belief that the backbone is the sole component of the fish's postcranial axial skeleton is the notion that the locomotory muscles pull only on the backbone. We point out that in the locomotory muscles of sharks—and presumably of many bony fishes as well—each muscle segment attaches to the skin over an area similar to that by which it attaches to the backbone. Compared to a muscle fiber near the backbone, a muscle fiber next to the midlateral skin must shorten more but with less force to produce the same degree of spinal flexure. Thus the skin of a shark is a tendon that increases the mechanical advantage of the locomotory muscle. Most tendons act in series with the muscles whose shortening and force they transmit. Shark skin transmits force in parallel with its attached, underlying muscle. The energy storage gained by the elastic deformation of a tendon of a given cross-sectional area is proportional to its length, hence the advantage of long tendons in ungulates (*11*). Sharks, and perhaps many bony fish, have their vast locomotory musculature entrained with the skin that acts as a whole-body tendon extending from the cranium to the tail end of the backbone.

If the shark's skin is to transmit forces of contracting muscles to the tail, the skin must be stiff for the duration of muscle contraction. Our findings lead us to the following interpretation: At rest, the muscles on both sides of the fish have the same length and cross-sectional area, and the fibers in the skin make a 60° angle with the fish's long axis. Internal pressure is low and so is skin stiffness.

To bend sharply as in fast swimming, the muscle on one side shortens and increases in cross-sectional area and girth. This causes fibers in the skin overlying the contracting muscles to increase their angle. The fiber angle controls the change in girth per unit change in length of the skin in concert with the surface of the contracting muscle. The changes in fiber angle imposed by the muscle causes the skin to remain taut in containing the muscle volume and to avoid wrinkling or loss of tension on the concave side of the fish.

Contracting muscle pulls on myosepta that pull on the skin and backbone. Since skin stiffness is high, tensile forces applied to it are transmitted by it from the head to the tail. Since the backbone resists compressive changes in the fish's body length, contracting muscles pull on one side of the head and tail causing the fish to bend rather than to shorten. The importance of the skin as an exotendon that transmits muscular force and displacement is, we believe, noteworthy.

S. A. WAINWRIGHT
F. VOSBURGH
J. H. HEBRANK
Zoology Department, Duke University, Durham, North Carolina 27706 and
Duke University Marine Laboratory, Beaufort, North Carolina 28516

References and Notes

1. We placed the point of a 19-gauge hypodermic needle attached to a Kulite semiconductor pressure transducer under the skin between the first and second dorsal fins half way between the lateral line and the middorsal septum. The lead was fixed to the first dorsal fin and led off to a Brush 220 chart recorder. The lead allowed the fish to resume its habitual swimming around the perimeter of a tank (8 m in diameter by 1.6 m depth) at Marineland, Inc., St. Augustine, Fla. All measurements of curvature and skin deformations were made from motion pictures taken with a Canon Scoopic 16-mm camera operated at 48 frames per second and analyzed with the aid of a Perceptoscope.
2. J. F. Daniel, *The Elasmobranch Fishes* (Univ. of California Press, Berkeley, 1928).
3. P. J. Motta, *Copeia* (1977), p. 454.
4. Six blacknose (*Carcharinus acronotus*), one dusky (*C. obscurus*), one spinner (*C. maculipinnis*), one sharpnose (*Rhizoprionodon terraenovae*), and one Florida smoothhound (*Mustelus norrisi*) were caught off Beaufort, N.C., and three lemon sharks were caught off St. Augustine, Fla. Pushing a sharp object to dent the lateral skin of a living or freshly dead shark causes two intersecting grooves to appear in the skin. These grooves radiate from the pressure point. We measured the azimuth of the grooves on the shark and, after having confirmed by dissection that the groove azimuth was the fiber azimuth on three sharks, we assumed all further groove azimuths to be fiber azimuths.
5. F. Vosburgh and J. H. Hebrank, in preparation.
6. S. A. Wainwright, W. D. Biggs, J. D. Currey, J. M. Gosline, *Mechanical Design in Organisms* (Arnold, Halsted, N.Y., 1976), pp. 180 and 293-298.
7. Stress in the skin = pr/t, where p = pressure, r = radius of cylinder, and t = skin thickness.
8. Samples were secured by snap swivels passing through holes in the sample edges. Wire fishing leaders connected the snap swivels to four sets of binding posts mounted 90° apart in the plane of the specimen. The use of point attachments permitted individual adjustment of tension in the wires and allowed stretch in the orthogonal direction. Two sets of binding posts were mounted to sliding carriages whose motions were controlled by lead screws and which caused extension of the sample. Extension in each direction was measured as the net movement between two pins stuck lightly in the sample. The pins drove the cores of colinear Linear Variable Differential Transducers. Force was held constant by monitoring sensor output and by adjusting the appropriate lead screw. Samples were bathed with fresh seawater during the experiments.
9. Skin deformation was metered by two thumbtacks stuck through a piece of flexible white plastic (0.5 mm thick by 15 mm wide by 80 to 150 mm long) into the skin of the shark. One tack held the skin and plastic in register while the other tack was attached to the skin but free to ride back and forth in a slot cut in the plastic. The length of the plastic and the distance between the tacks were measured on projected motion picture images, and the ratio of the intertack distance to length of plastic was computed for every fourth frame.
10. A. M. Gordon, A. F. Huxley, F. J. Julian, *J. Physiol. (London)* **184**, 170 (1966); B. C. Abbott and D. R. Wilkie, *ibid.* **120**, 214 (1953).
11. R. McN. Alexander and H. C. Bennet-Clark, *Nature (London)* **265**, 114 (1977).
12. We thank the staffs of the Duke University Marine Laboratory, the Cornelius Vanderbilt Whitney Laboratory of the University of Florida and Marineland, Inc., for services, hospitality, and unstinting cooperation. M. R. Hebrank gave vital assistance in every phase of the study. Prof. J. E. Gordon gave fruitful discussion and suggested we study torsion.

13 March 1978; revised 31 May 1978

Acoustic Detection of Cosmic-Ray Air Showers

Abstract. *The signal strength, bandwidth, and detection range of acoustic pulses generated by cosmic-ray air showers striking a water surface are calculated. These signals are strong enough to be audible to a submerged swimmer. The phenomena may be useful for studying very-high-energy cosmic rays and may help answer the important question of whether the origin of cosmic rays is extragalactic or galactic.*

Extensive air showers (EAS) created by cosmic rays with energies greater than 10^{19} eV (approximately 1 calorie) are predicted to occur with a frequency of 1.5×10^{-9} m^{-2} day^{-1} sr^{-1} (*1*). Obviously a large detector is required to observe these events with any regularity. I will show here that large bodies of water will convert this energy into a detectable acoustic signal and that these events are probably being detected, as undesired background noise by U.S. Navy fixed underwater acoustic installations used for the calibration of equipment and the measurement of underwater acoustic signals and spectra (*2*).

Table 1. Calculated detection range for an acoustic signal generated by the nuclear-active components of an EAS with energy $E_0 = 10^{19}$ eV.

Frequency	Sea state	Detection range (km)		
		0 dB	6 dB	20 dB
100 Hz	6	0.03	0.01	0.004
	0	0.2	0.1	0.02
1 kHz	6	0.02	0.01	0.004
	0	0.4	0.2	0.04
10 kHz	6	0.1	0.06	0.01
	0	2.0	1.2	0.3
30 kHz	6	0.3	0.2	0.04
	0	1.6	1.2	0.4
100 kHz	6	0.3	0.2	0.07
	0	0.5	0.4	0.2

The source of cosmic-ray particles is an important unanswered question. Cosmic-ray protons with energies much greater than 10^{21} eV should not exist if their origin is extragalactic (*3*), since they lose energy through interactions with low-energy photons which constitute the 3°K universal background radiation. Events of this energy occur about 100 times less frequently than the 10^{19}-eV events. The largest instruments presently used will detect events above 10^{21} eV so rarely that their data will be inconclusive. The acoustic detection technique should determine the presence or absence of very-high-energy, cosmic-ray particles.

An EAS has three principal components (*3*). The first is the nuclear-active particle core containing about $^1/_8$ of the total energy in a radius of 10 m. The second is the electron component, with about the same fraction of the total energy as the nuclear component. Half of the electrons strike within a 50-m radius of the core. The third component, the muons, contain about $^3/_4$ of the total energy; one half of the muons strike within about 320 m of the core. The more energetic particles strike closer to the core. It